

Supplement of

Solar Radiation Modification hampers decarbonization with renewable solar energy

Susanne Baur et al.

Correspondence to: Susanne Baur (susanne.baur@cerfacs.fr)

Table S1: Constants and variables used for calculation of technical PV and CSP potential

Symbol	Description	Value	Reference
$RSDS$	Downwelling shortwave radiation	[W m ⁻²]	model output
$RSDS_{dir}$	Downwelling direct shortwave radiation	[W m ⁻²]	model output
h	Hours in a year	8670 [h]	-
A	Suitability factor	0-1	-
a	Area of grid cell	[m ²]	-
n_{LPV}	PV land use factor	47 %	Köberle et al., 2015; Ong et al., 2013
n_{LCSP}	CSP land use factor	37 %	Köberle et al., 2015; Trieb et al., 2009
n_{PV}	PV panel efficiency corrected for atmospheric variables	-	-
n_{panel}	PV panel efficiency under STC	26.8 %	Fraunhofer ISE, 2023; NREL, 2023
n_{CSP}	CSP efficiency corrected for atmospheric variables	-	-
T_p	PV panel temperature	[°C]	-
T	Surface air temperature	[°C]	model output
T_{STC}	PV panel temperature under STC	25 [°C]	Crook et al., 2011
T_f	Fluid temperature in the absorber	115 °C	Dudley 1995; Crook et al., 2011; Dutta et al., 2022; Wild et al., 2017; Gernaat et al., 2021
c_1		4.3 [°C]	Crook et al., 2011; Dutta et al., 2022; Gernaat et al., 2021
c_2		0.943	Crook et al., 2011; Dutta et al., 2022; Gernaat et al., 2021
c_3		0.028 [°C m ² W ⁻¹]	Crook et al., 2011; Dutta et al., 2022; Gernaat et al., 2021
c_4		-1.528 [°Csm ⁻¹]	Crook et al., 2011; Dutta et al., 2022; Gernaat et al., 2021

Symbol	Description	Value	Reference
RS_{DS}	Downwelling shortwave radiation	[W m ⁻²]	model output
$RS_{DS_{dir}}$	Downwelling direct shortwave radiation	[W m ⁻²]	model output
h	Hours in a year	8670 [h]	-
V	Surface wind velocity	[ms ⁻¹]	model output
PR	Performance ratio	85 %	Fraunhofer ISE, 2023
γ	Efficiency response of mono-silicone PV panels	-0.005 [°C ⁻¹]	Dutta et al., 2022; Jerez et al., 2015; Sawadogo et al., 2021; Feron et al., 2021
n_R	Rankine cycle efficiency	40 %	Gernaat et al., 2021
FLH	Full Load Hours	h	-
k_0	-	0.762	Crook et al., 2011; Dudley 1995; Wild et al., 2017; Dutta et al., 2022; Gernaat et al., 2021
k_1	-	0.2125 [W m ⁻² °C ⁻¹]	Crook et al., 2011; Dudley 1995; Wild et al., 2017; Dutta et al., 2022; Gernaat et al., 2021

Table S2: land use suitability fractions

Land use / land cover category	Reference suitability value for PV & CSP
Agricultural land	1 %
Extensive grassland	5 %
Carbon plantation	0
Regrowth forest abandoning	0
Regrowth forest timber	0
Biofuels	0
Ice	0
Tundra	10 %
Wooded tundra	0
Boreal forest	0
Cool conifer forest	0
Temp. mixed forest	0
Temp decid. forest	0
Warm mixed forest	0
Grassland / steppe	10 %
Hot desert	25 %
Scrubland	10 %

Savannah	8 %
Tropical woodland	0
Tropical forest	0

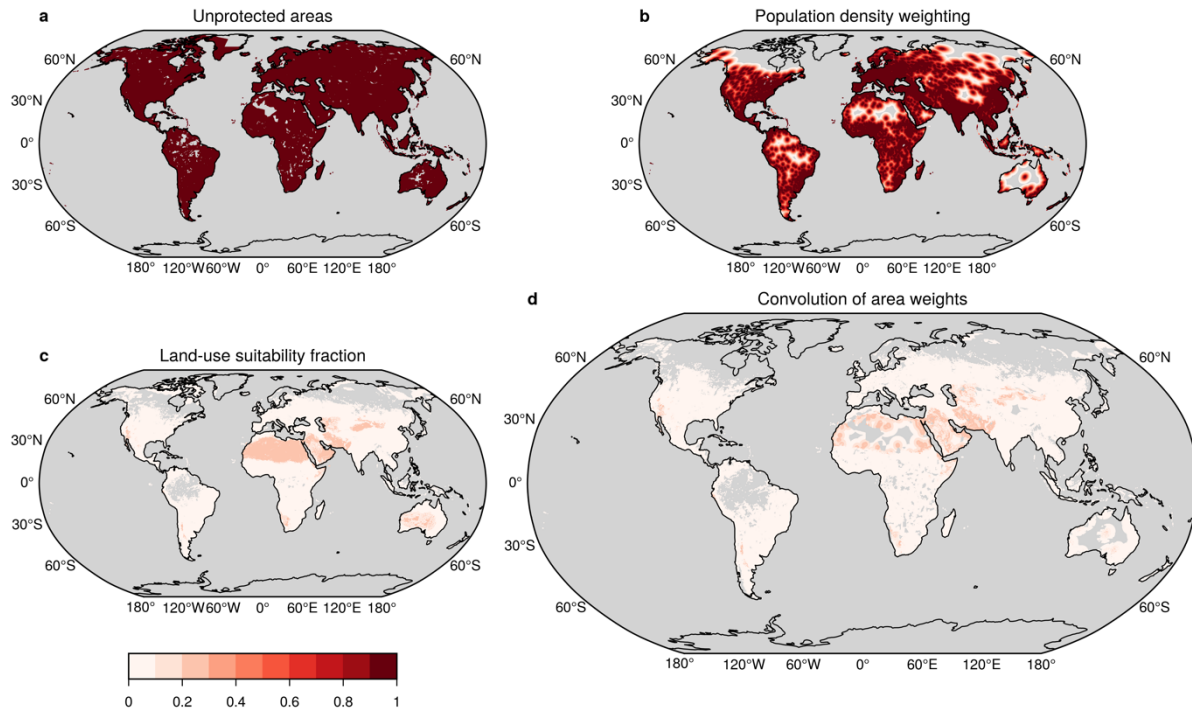


Figure S1: Conceptual figure of the single weights used for area weighting of the technical potential. a) unprotected areas (IUCN), b) weighting of distance to densely populated areas (Stehfest et al., 2014; Doelman et al., 2018), c) weighting according to land use cover (Stehfest et al., 2014; Doelman et al., 2018) and d) convolution of a, b and c.

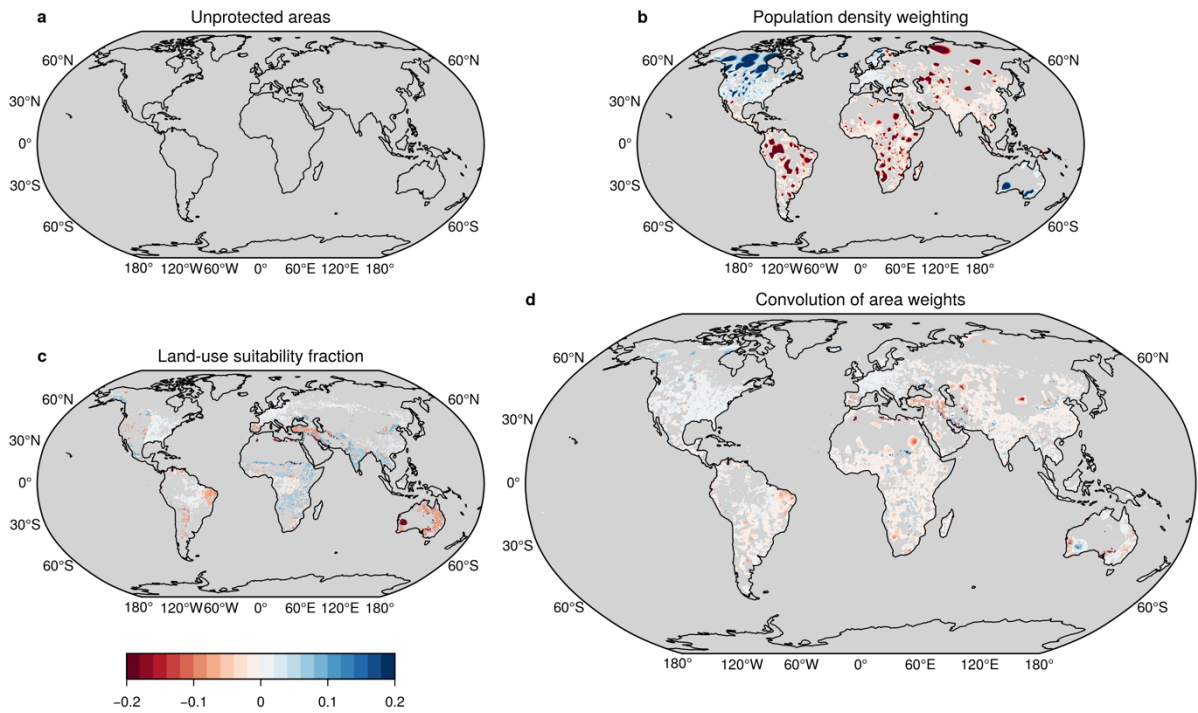


Figure S2: Difference in area weighting between *ssp245* and *ssp585* for a) unprotected areas (IUCN), b) weighting of distance to densely populated areas (Stehfest et al., 2014; Doelman et al., 2018), c) weighting according to land use cover (Stehfest et al., 2014; Doelman et al., 2018) and d) convolution of a, b and c.

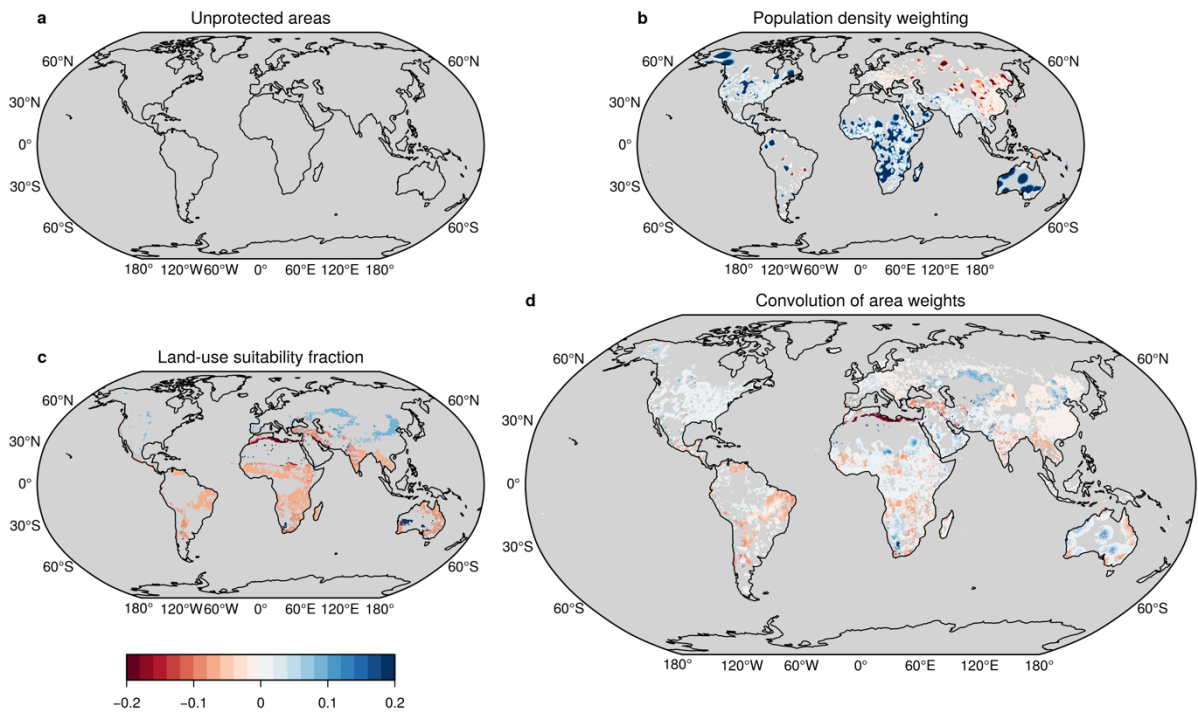


Figure S3: Difference in *ssp2* area weighting between the present (2015-2024) and the future (2090-99) for a) unprotected areas (IUCN), b) weighting of distance to densely populated areas (Stehfest et al., 2014; Doelman et al., 2018), c) weighting according to land use cover (Stehfest et al., 2014; Doelman et al., 2018) and d) convolution of a, b and c.

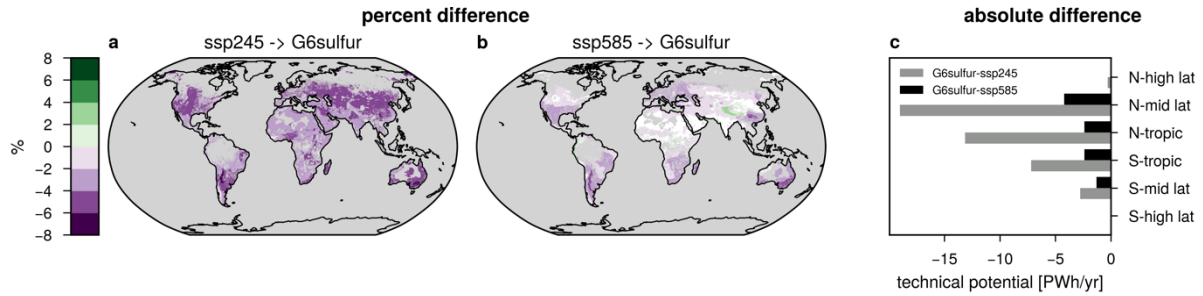


Figure S4: Difference in PV (a-c) and CSP (d-f) technical potential between the ensemble means of G6sulfur and a,d) ssp245, b,e) ssp585 and c,f) absolute difference between latitudinal zonal sums between G6sulfur and ssp245 and ssp585 in PWh/year using land-use suitability factors according to scenario (ssp2 for ssp245; ssp5 for ssp585 and G6sulfur). White areas have a SNR of < 1. Relative differences are constrained to areas considered suitable under ssp245 and ssp585. Areas that are relevant under G6sulfur but not ssp245 are therefore not displayed.

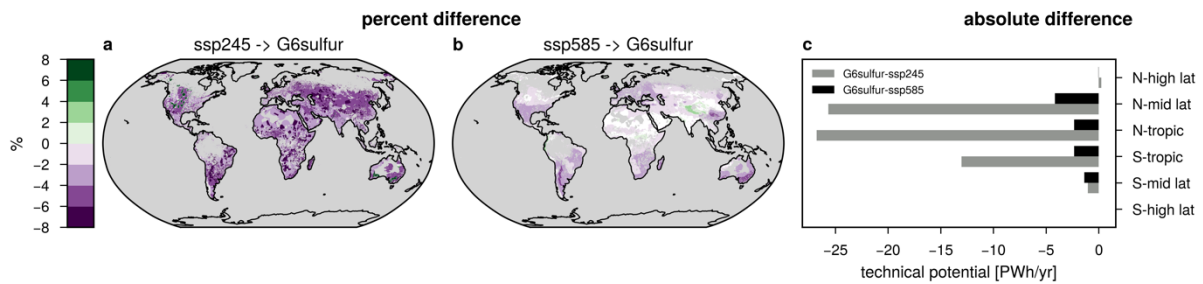


Figure S5: Difference in PV (a-c) and CSP (d-f) technical potential between the ensemble means of G6sulfur and a,d) ssp245, b,e) ssp585 and c,f) absolute difference between latitudinal zonal sums between G6sulfur and ssp245 and ssp585 in PWh/year using land-use suitability factors and population density assumptions according to scenario (ssp2 for ssp245; ssp5 for ssp585 and G6sulfur). White areas have a SNR of < 1. Relative differences are constrained to areas considered suitable under G6sulfur. Relative differences are constrained to areas considered suitable under ssp245 and ssp585. Areas that are relevant under G6sulfur but not ssp245 are therefore not displayed.

Table S3: Total global CSP technical potential per scenario in PWh/yr under different geographical constraints but always with the minimum-radiation-requirement constraint.

Geographical constraints	G6sulfur	ssp585	ssp245
Land areas	1,026	1,705	1,679
Unprotected areas on land	859	1,449	1,430
Unprotected areas on land weighted with suitability fractions	126	163	163
Unprotected areas on land weighted with suitability fractions and distance to highly populated areas	73	99	99

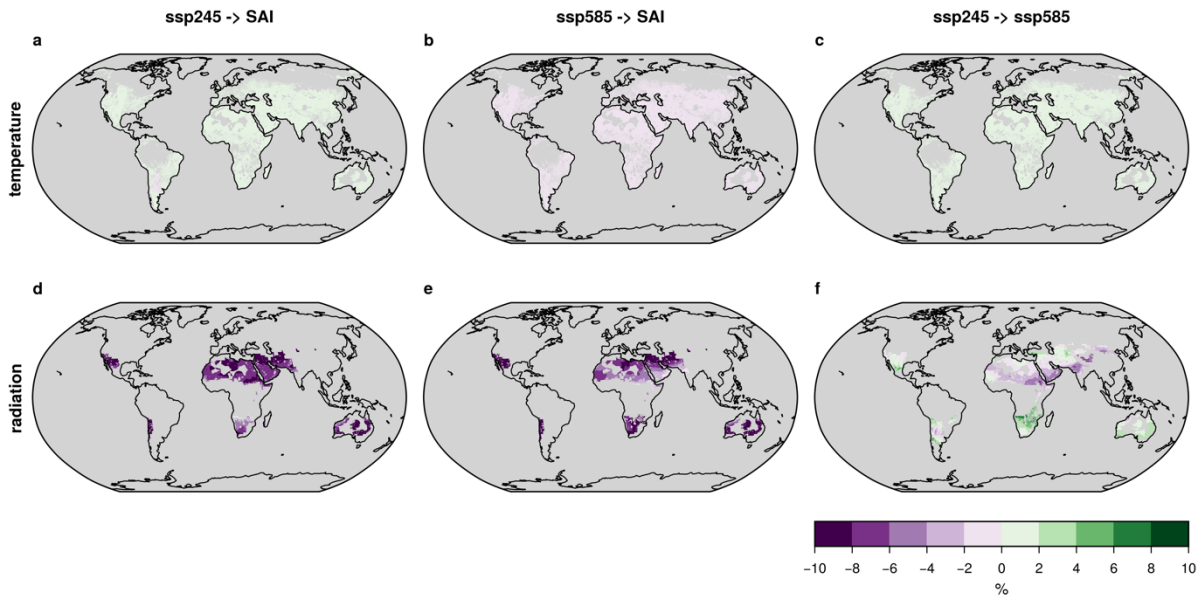


Figure S6: Main drivers of change in 2090-2099 CSP potential, a,b,c) surface air temperature and d-f) total downwelling direct surface radiation. Areas with SNR < 1 are shown in white.

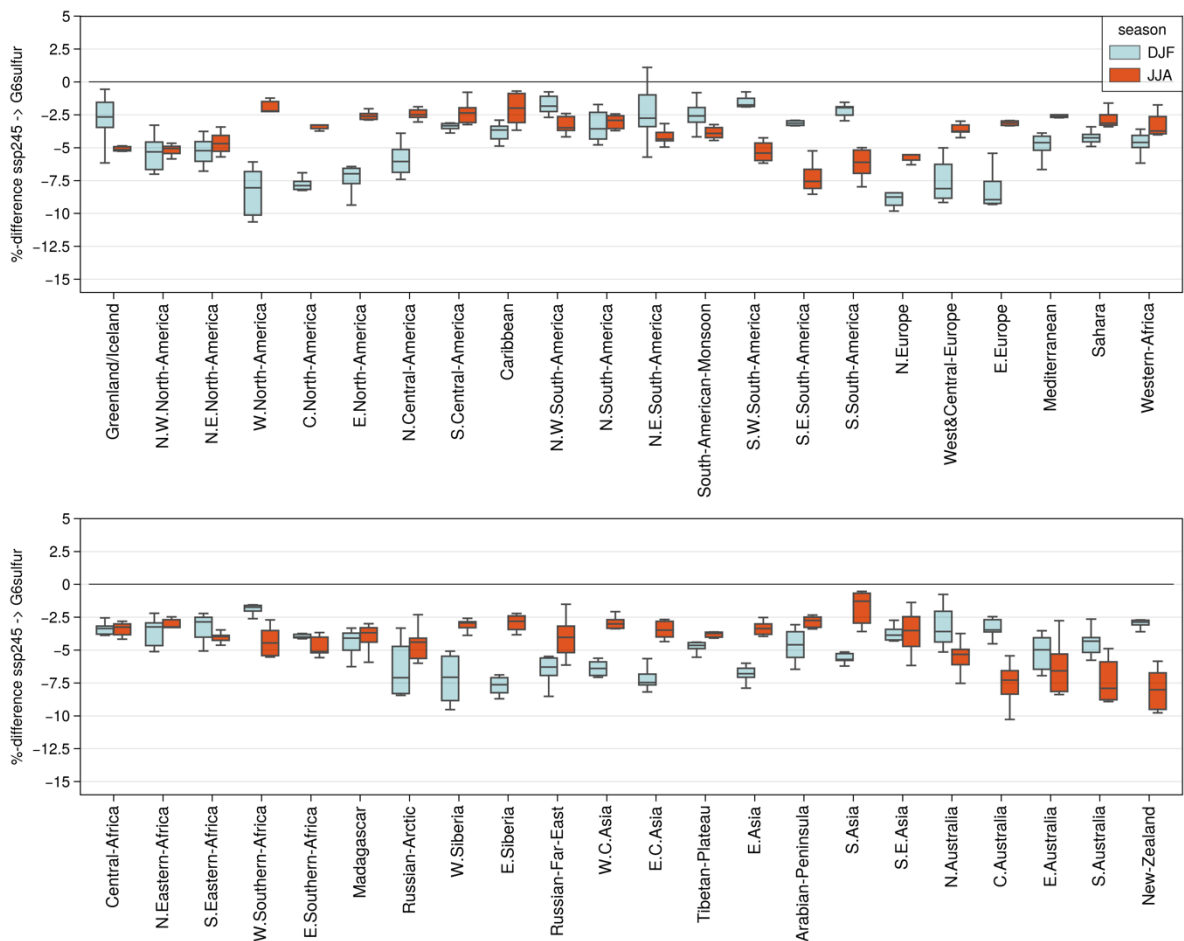


Figure S7: Relative change in 2090-99 PV potential from ssp245 to G6sulfur for all IPCC AR6 regions except Antarctica (Iurbide et al., 2020) split up into two seasons of December, January, February (lightblue) and June, July, August (orangered). Range over boxplot represents the spread over the 6 ensemble members.

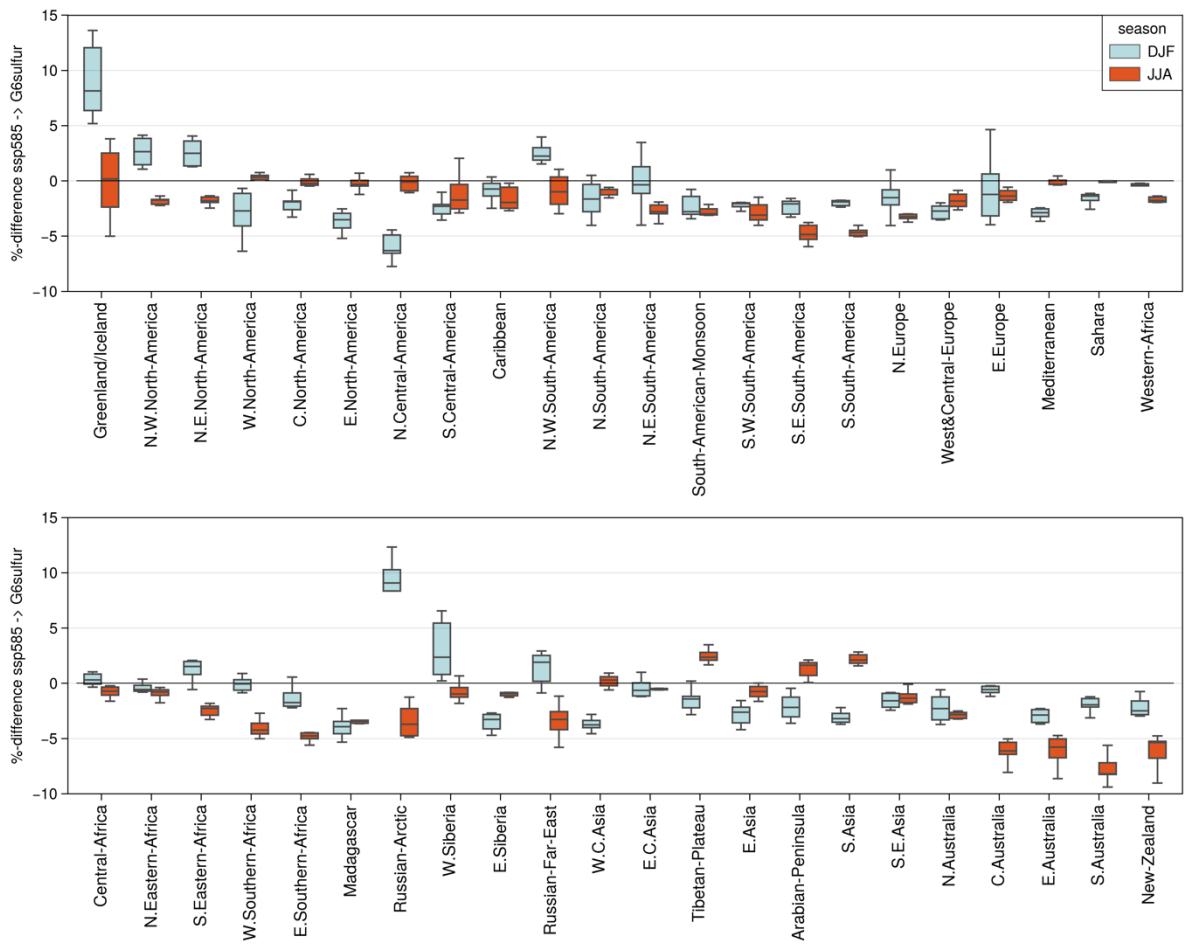


Figure S8: Relative change in 2090-99 PV potential from ssp585 to G6sulfur for all IPCC AR6 regions except Antarctica (Iturbide et al., 2020) split up into two seasons of December, January, February (lightblue) and June, July, August (orange). Range over boxplot represents the spread over the 6 ensemble members.

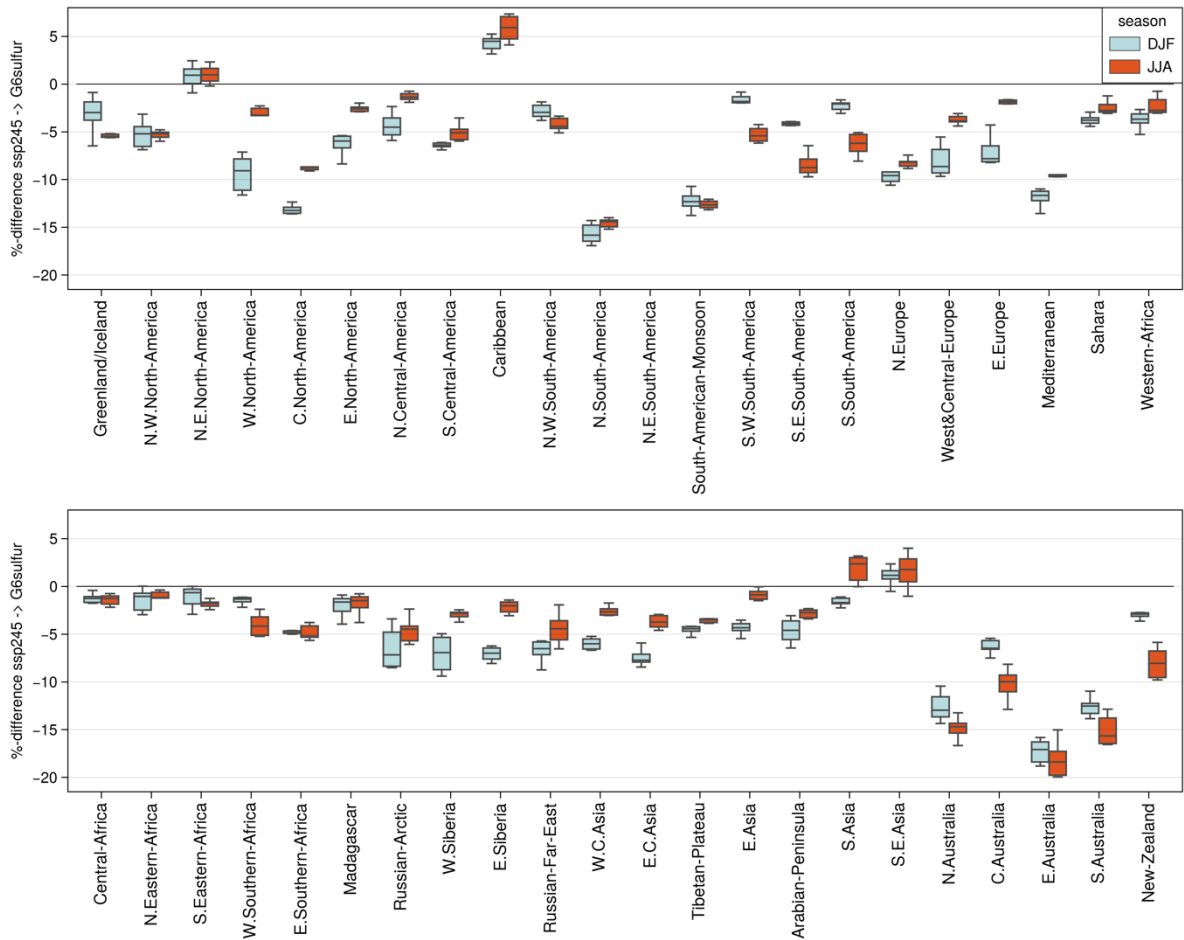


Figure S9: Relative change in 2090-99 PV potential using land-use suitability factors according to scenario (ssp2 for ssp245; ssp5 G6sulfur) from ssp245 to G6sulfur for all IPCC AR6 regions except Antarctica (Iturbide et al., 2020) split up into two seasons of December, January, February (lightblue) and June, July, August (orangered). Range over boxplot represents the spread over the 6 ensemble members.

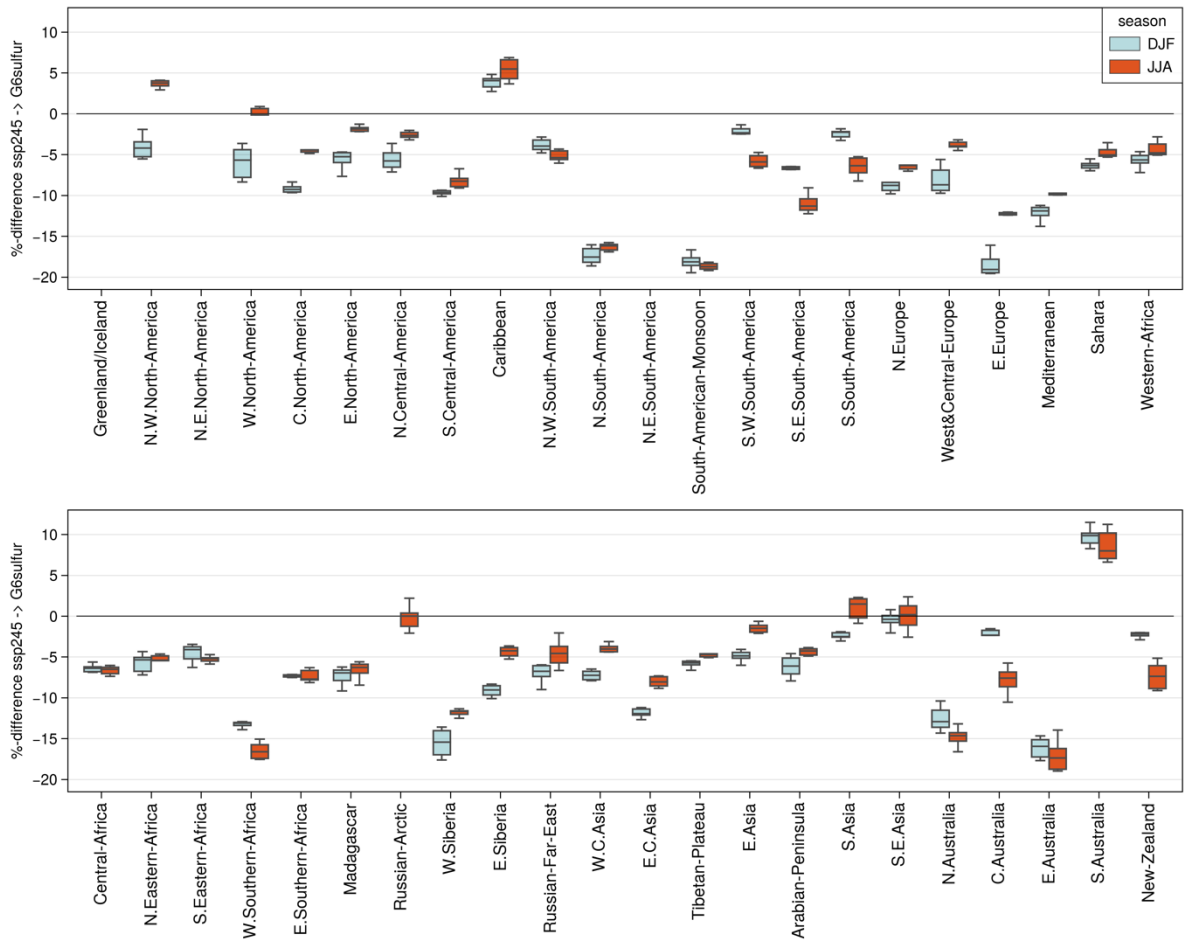


Figure S10: Relative change in 2090-99 PV potential using land-use suitability factors and population density according to scenario (ssp2 for ssp245; ssp5 G6sulfur) from ssp245 to G6sulfur for all IPCC AR6 regions except Antarctica (Iturbide et al., 2020) split up into two seasons of December, January, February (light-blue) and June, July, August (orange-red). Range over boxplot represents the spread over the 6 ensemble members.

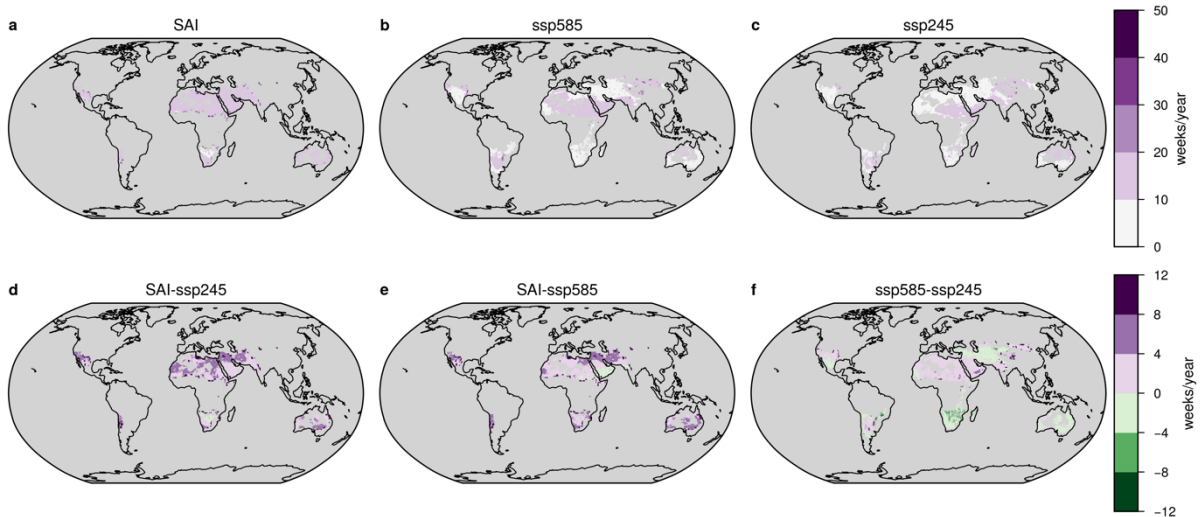


Figure S11: CSP Low Energy Week metric for a) G6sulfur, b) ssp585 and c) ssp245. The LEW is calculated between the present (2015-2019) and the future (2095-2099) with equal area weighting. See 2.3 for the LEW equation.

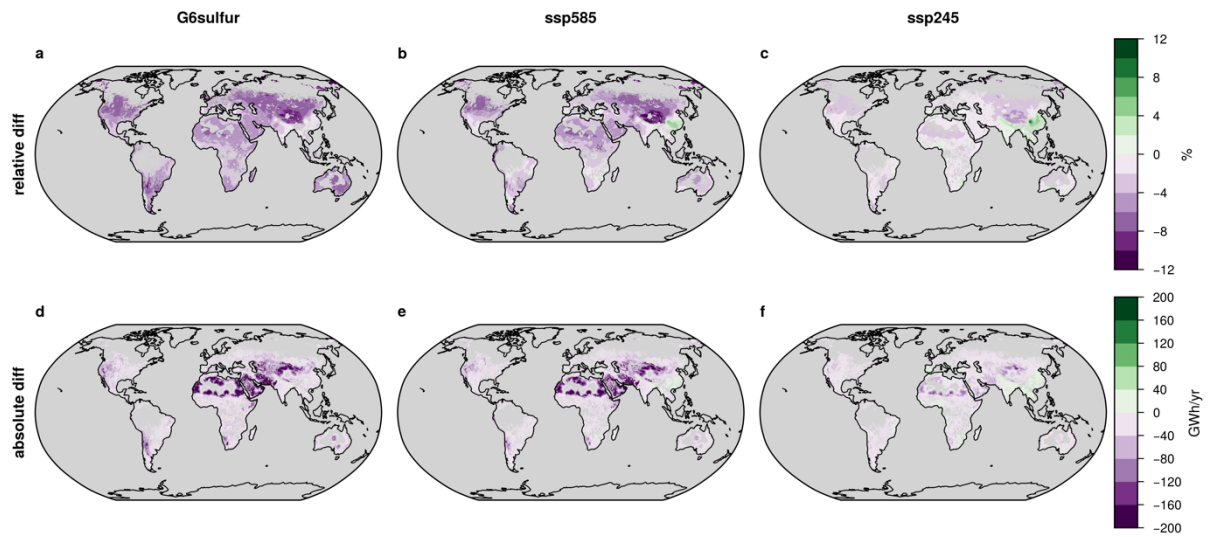


Figure S12: Comparing present (2015-2024) versus future (2090-2099) in relative (a-c) and absolute (d-f) terms for G6sulfur (a,d), ssp585 (b,e) and ssp245 (c,f) using constant area weighting.

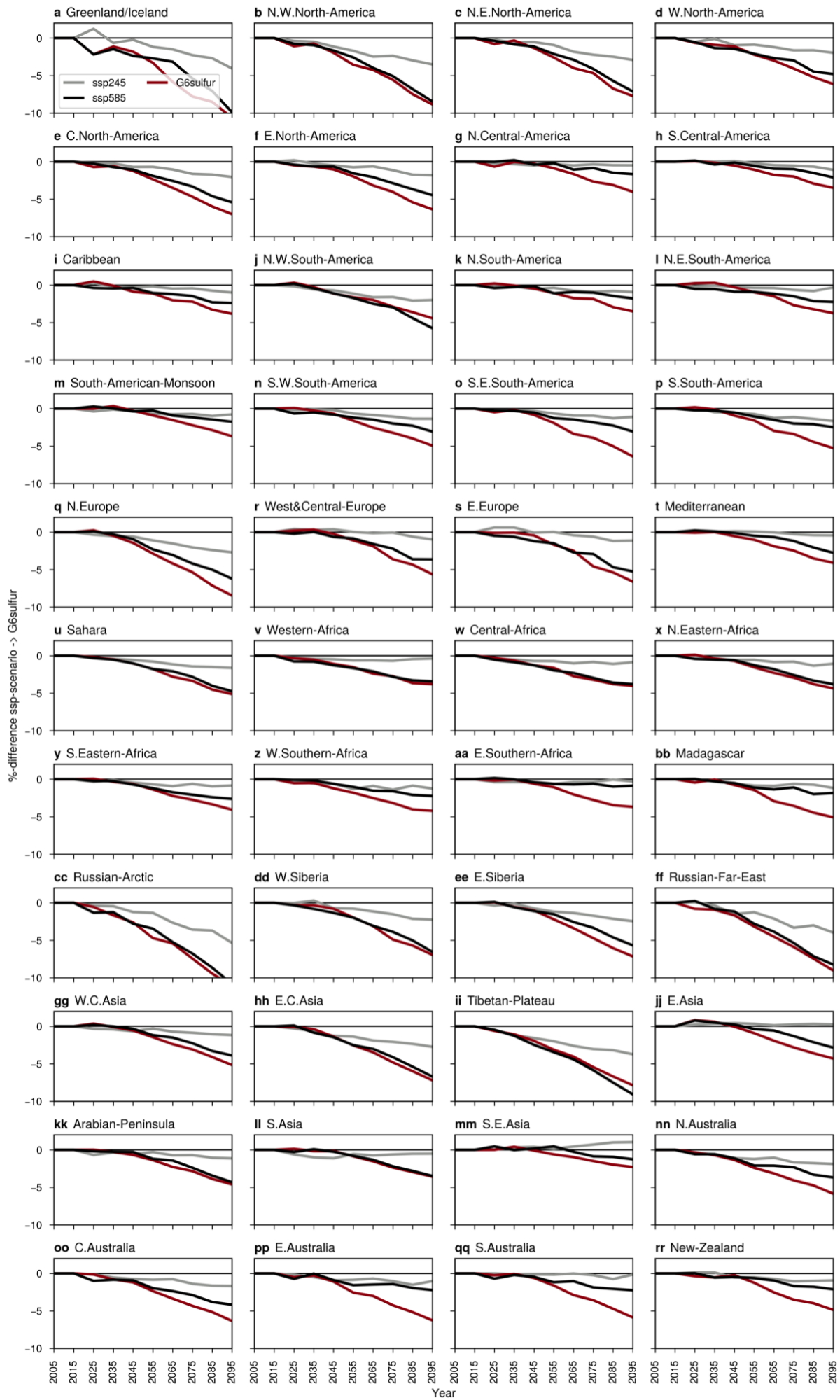


Figure S13: Relative difference over time of G6sulfur (red), ssp245 (gray) and ssp585 (black) PV potential compared to 2015-2024 values. Lines are the ensemble means with the bars indicating the 20-80 percentile ranges of the single members.

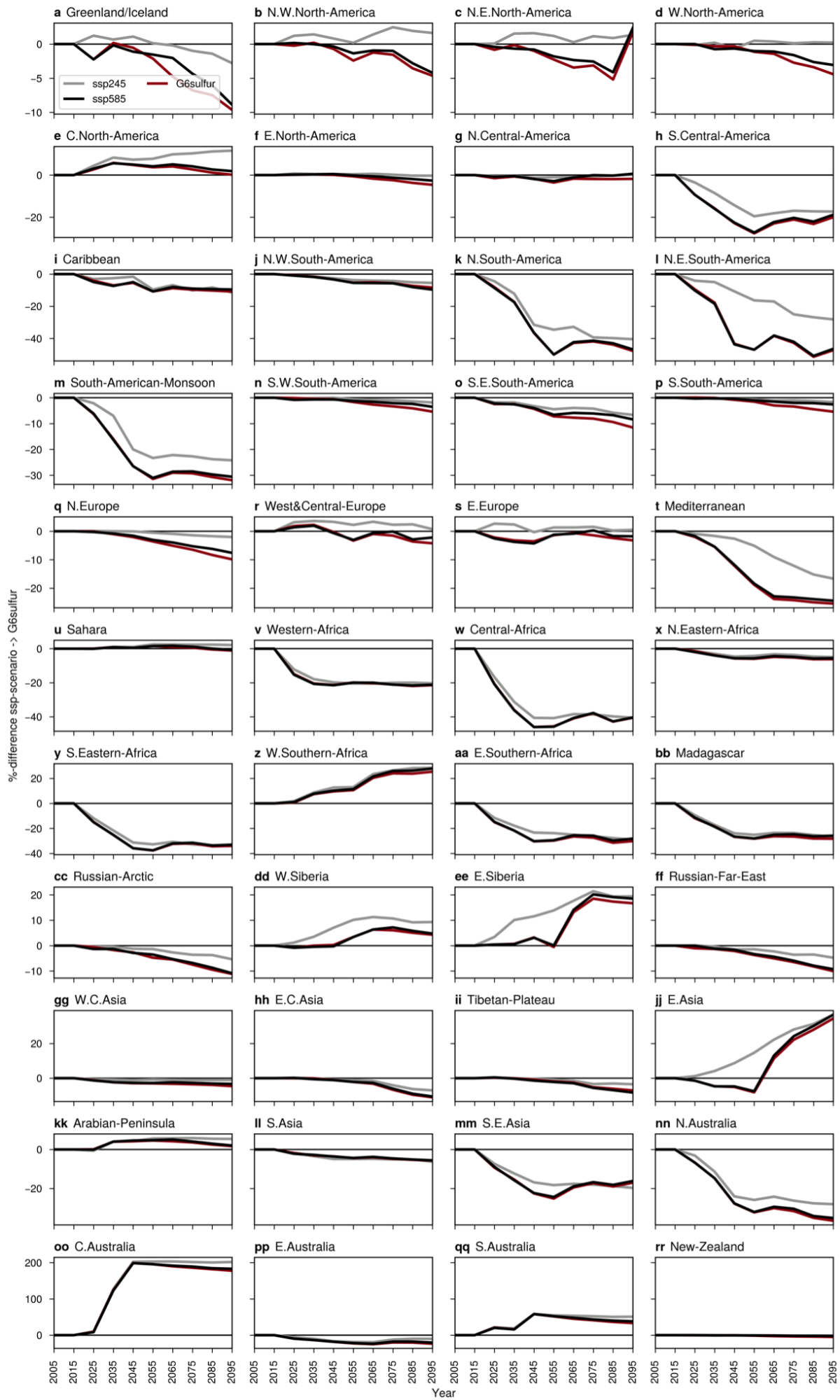


Figure S14: Relative difference over time of G6sulfur (red), ssp245 (gray) and ssp585 (black) PV potential compared to 2015-2024 values. Land-use suitability weighting according to scenario. Lines are the ensemble means with the bars indicating the 20-80 percentile ranges of the single members.

References:

- Crook, J. A., Jones, L. A., Forster, P. M., and Crook, R.: Climate change impacts on future photovoltaic and concentrated solar power energy output, *Energy and Environmental Science*, 4, 3101–3109, <https://doi.org/10.1039/c1ee01495a>, 2011.
- Doelman, J. C., Stehfest, E., Tabeau, A., Van Meijl, H., Lassaletta, L., Gernaat, D. E. H. J., Hermans, K., Harmsen, M., Daioglou, V., Biemans, H., Van Der Sluis, S., and Van Vuuren, D. P.: Exploring SSP land-use dynamics using the IMAGE model: Regional and gridded scenarios of land-use change and land-based climate change mitigation, *Global Environmental Change*, 48, 119–135, <https://doi.org/10.1016/j.gloenvcha.2017.11.014>, 2018.
- Dudley, V.: SANDIA Report test results for industrial solar technology parabolic trough solar collector, SAND-94-1117, Albuquerque, USA: Sandia National Laboratory, 1995.
- Dutta, R., Chanda, K., and Maity, R.: Future of solar energy potential in a changing climate across the world: A CMIP6 multi-model ensemble analysis, *Renewable Energy*, 188, 819–829, <https://doi.org/10.1016/j.renene.2022.02.023>, 2022.
- Fraunhofer ISE: Photovoltaics report, Fraunhofer Institute for Solar Energy Systems, <https://www.ise.fraunhofer.de/content/dam/ise/de/documents/publications/studies/Photovoltaics-Report.pdf>, 2023.
- Gernaat, D. E. H. J., de Boer, H. S., Daioglou, V., Yalaw, S. G., Müller, C., and van Vuuren, D. P.: Climate change impacts on renewable energy supply, *Nature Climate Change*, 11, 119–125, <https://doi.org/10.1038/s41558-020-00949-9>, 2021.
- Iturbide, M., Gutiérrez, J. M., Alves, L. M., Bedia, J., Cerezo-Mota, R., Cimadevilla, E., Cofiño, A. S., Di Luca, A., Faria, S. H., Gorodetskaya, I. V., Hauser, M., Herrera, S., Hennessy, K., Hewitt, H. T., Jones, R. G., Krakovska, S., Manzanas, R., Martínez-Castro, D., Narisma, G. T., Nurhati, I. S., Pinto, I., Seneviratne, S. I., van den Hurk, B., and Vera, C. S.: An update of IPCC climate reference regions for subcontinental analysis of climate model data: definition and aggregated datasets, *Earth System Science Data*, 12, 2959–2970, <https://doi.org/10.5194/essd-12-2959-2020>, 2020.
- IUCN (International Union for Conservation of Nature): The World Database on Protected Areas (WDPA), 2023.
- Jerez, S., Tobin, I., Vautard, R., Montávez, J. P., López-Romero, J. M., Thais, F., Bartok, B., Christensen, O. B., Colette, A., Déqué, M., Nikulin, G., Kotlarski, S., Van Meijgaard, E., Teichmann, C., and Wild, M.: The impact of climate change on photovoltaic power generation in Europe, *Nature Communications*, 6, <https://doi.org/10.1038/ncomms10014>, 2015.
- Köberle, A. C., Gernaat, D. E. H. J., and van Vuuren, D. P.: Assessing current and future techno-economic potential of concentrated solar power and photovoltaic electricity generation, *Energy*, 89, 739–756, <https://doi.org/10.1016/j.energy.2015.05.145>, 2015.
- NREL (National Renewable Energy Laboratory): Best Research-Cell Efficiency Chart, National Renewable Energy Laboratory, <https://www.nrel.gov/pv/cell-efficiency.html> (last accessed: August 2023), 2023.
- Ong, S., Campbell, C., Denholm, P., Margolis, R., and Heath, G.: Land-Use Requirements for Solar Power Plants in the United States, <https://doi.org/10.2172/1086349>, 2013.

Sawadogo, W., Reboita, M. S., Faye, A., da Rocha, R. P., Odoulami, R. C., Olusegun, C. F., Adeniyi, M. O., Abiodun, B. J., Sylla, M. B., Diallo, I., Coppola, E., and Giorgi, F.: Current and future potential of solar and wind energy over Africa using the RegCM4 CORDEX-CORE ensemble, *Clim Dyn*, 57, 1647–1672, <https://doi.org/10.1007/s00382-020-05377-1>, 2021.

Stehfest, E., Van Vuuren, D., Kram, T., Bouwman, L., Alkemade, R., Bakkenes, M., Biemans, H., Bouwman, A., Den Elzen, M., Janse, J., Lucas, P., Van Minnen, J., Müller, C., Prins, A.: Integrated Assessment of Global Environmental Change with IMAGE 3.0. Model Description and Policy Applications, Netherlands Environmental Assessment Agency (The Hague), ISBN: 978-94-91506-71-0, 2014.

Trieb, F., Schillings, C., O’Sullivan, M., Pregger, T., and Hoyer-Klick, C.: Global Potential of Concentrating Solar Power, 11, 2009.

Wild, M., Folini, D., and Henschel, F.: Impact of climate change on future concentrated solar power (CSP) production, RADIATION PROCESSES IN THE ATMOSPHERE AND OCEAN (IRS2016): Proceedings of the International Radiation Symposium (IRC/IAMAS), Auckland, New Zealand, 100007, <https://doi.org/10.1063/1.4975562>, 2017.